Synthesis and Structural Trends in Pentafluorophenyl-Substituted Ferrocenes, 1,4-Tetrafluorophenylene-Linked Diferrocenes, and 1,1′-Ferrocenylene−1,4-Tetrafluorophenylene Co-oligomers

Paul A. Deck,* Michael J. Lane,[1] Jennifer L. Montgomery,[1] and Carla Slebodnick

Department of Chemistry, Virginia Tech, Blacksburg, Virginia 24061-0212

Frank R. Fronczek

Department of Chemistry, Louisiana State University, Baton Rouge, Louisiana 70803-1804

Received November 26, 1999

1,1′-Dilithioferrocene, or $(CpLi)_2Fe$ (**1**), reacts with excess C_6F_6 in THF to afford mostly $(C_6F_5Cp)_2Fe$ (**2**), accompanied by the diiron complex $(C_6F_5Cp)FeCp(1,4\text{-}C_6F_4)CpFe(CpC_6F_5)$ (**3**). The reaction of **1** with 1.0 equiv of C_6F_6 affords a mixture of sparingly soluble step-growth oligomers assigned to $[-FeCp(1,4\text{-}C_6F_4)-]_n$ (**4**). [1-Li-2-R^NCp]FeCp (**6**, $R^N = CH_2NMe_2$) reacts with 1 equiv of C_6F_6 to afford [1-(C_6F_5)-2-R^NCp]FeCp (**7**). Complex **6** reacts with 0.5 equiv of C_6F_6 to afford CpFe[2-R^NCp](1,4-C_6F_4)[2-R^NCp]FeCp as a mixture of two diastereomers (***meso*-8**, major and ***dl*-8**, minor). The relative stereochemistry of ***meso*-8** is established by crystallographic analysis of the corresponding bis(methiodide) (**12**). [1-Li-2-R^NCp]Fe(CpLi) (**9**) reacts with excess C_6F_6 to afford mainly the diarylated ferrocene [1-(C_6F_5)-2-R^NCp]Fe(CpC_6F_5) (**10**). The reaction of **9** instead with 1.0 equiv of C_6F_6 affords a mixture of oligomeric species assigned to the formula $[-(2\text{-}R^NCp)FeCp(1,4\text{-}C_6F_4)-]_n$ (**11**). In contrast to **4**, **11** is sufficiently soluble for characterization by solution NMR spectroscopy (end group analysis), and under optimized conditions a number-averaged degree of oligomerization corresponding to a linear Fe_9 species is determined. The complexes **3**, **7**, **10**, and **12** are characterized by single-crystal X-ray diffraction. Crystalline **3** exhibits infinite π-stacking interactions composed of intramolecular "triple-decker" $C_6F_5-C_6F_4-C_6F_5$ stacking and intermolecular $Cp-C_6F_5$ stacking. The crystal structure of **10** also shows intramolecular arene stacking, but intermolecular $Cp-C_6F_5$ interaction is interrupted by the dimethylaminomethyl substituent. None of these complexes show intermolecular stacking among the various C_6F_5 and C_6F_4 groups. Extensive intermolecular C−H···F−C interactions in the crystallographic packing diagrams of **3**, **7**, **10**, **12**, and $CpFeCpC_6F_4C_6F_4CpFeCp$ (**13**) are characterized as either "purposeful" or "diffuse" by examining correlations of their respective H···F distances and C−H···F angles. Solution voltammetry of **3** shows two unresolved, reversible $Fe^{II}|Fe^{III}$ couples, suggesting weak electronic communication between the two iron centers despite the fully conjugated structure.

Introduction

Ferrocene-containing oligomers and polymers in which the complexed iron atoms are integral to the principal chain are under extensive investigation in several laboratories.[2] The use of the $Fe^{II}|Fe^{III}$ couple as a charge carrier in conducting organic filaments or films is often mentioned as a potential application of these materials.[3] Evidence for interactions among ferrocene groups at the molecular level is usually sought with electrochemical or spectroscopic measurements.[2,3a,4] Ring-opening polymerization of heteroferrocenophanes is currently the most general synthetic approach to high molecular weight polymers.[2a−d] Other approaches lead to more fully conjugated species with lower molecular weights.[4,5]

(1) Undergraduate research participants.

(2) (a) Nguyen, P.; Gomez-Elipe, P.; Manners, I. *Chem. Rev.* **1999**, *99*, 1515. (b) Kingsborough, R. P.; Swager, T. M. *Prog. Inorg. Chem.* **1999**, *48*, 123. (c) Manners, I. *Angew. Chem., Int. Ed. Engl.* **1996**, *35*, 1602−1621. (d) Manners, I. *Adv. Organomet. Chem.* **1995**, *37*, 131−168. (e) Kurosawa, M.; Nankawa, T.; Nishihara, H. *Inorg. Chem.* **1999**, *38*, 5113. (f) Plenio, H.; Hermann, J.; Leukel, J. *Eur. J. Inorg. Chem.* **1998**, *12*, 2063. (g) Heo, R. W.; Somoza, F. B.; Randall, T. *J. Am. Chem. Soc.* **1998**, *120*, 1621. (h) Southard, G. E.; Curtis, M. D. *Organometallics* **1997**, *16*, 5618.

(3) (a) Pittman, C. U.; Carraher, C. E.; Zeldin, M.; Sheats, J. E.; Culbertson, B. M. *Metal-Containing Polymeric Materials*; Plenum: New York, 1996. (b) Buretea, M. A.; Tilley, T. D. *Organometallics* **1997**, *16*, 1507. (c) Yamamoto, T.; Morikita, T.; Maruyama, T.; Kubota, K.; Katada, M. *Macromolecules* **1997**, *30*, 5390.

(4) (a) Barlow, S.; O'Hare, D. *Chem. Rev.* **1997**, *97*, 637. (b) Hradsky, A.; Bildstein, B.; Schuler, N.; Schottenberger, H.; Jaitner, P.; Ongania, K.-H.; Wurst, K.; Launay, J.-P. *Organometallics* **1997**, *16*, 392−402. (c) Hirao, T.; Kurashina, M.; Aramaki, K.; Nishihara, H. *J. Chem. Soc., Dalton Trans.* **1996**, 2929−2933. (d) Ribou, A.-C.; Launay, J.-P.; Sachtleben, M. L.; Li, H.; Spangler, C. W. *Inorg. Chem.* **1996**, *35*, 3735−3740. (e) Stanton, C. E.; Lee, T. R.; Grubbs, R. H.; Lewis, N. S.; Pudelski, J. K.; Callstrom, M. R.; Erickson, M. S.; McLaughlin, M. L. *Macromolecules* **1995**, *28*, 8713−8721. (f) Hudson, R. D. A.; Foxman, B. M.; Rosenblum, M. *Organometallics* **1999**, *18*, 4098−4106.

10.1021/om990930v CCC: $19.00
Publication on Web 02/25/2000

Scheme 1

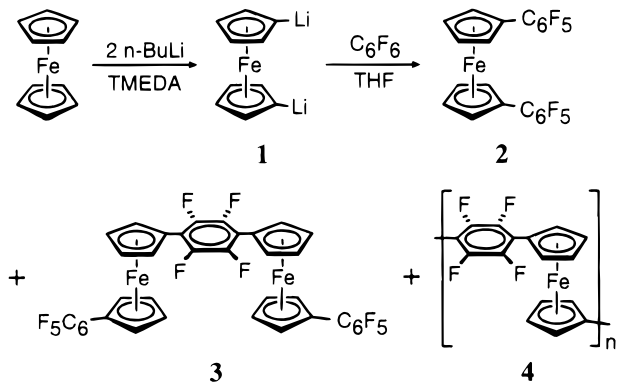

"Crystal engineering" is a rapidly growing area of research in which diverse combinations of intermolecular forces are orchestrated to enable rational syntheses of ordered solids,[6] including organometallic compounds.[7] Whereas hydrogen bonding remains the most important molecular recognition design factor, several groups have recently turned their attention toward weaker interactions, including those characteristic of organic fluorides.[8–10] Detailed understanding of these weaker forces stands to broaden the scope of crystal engineering concepts to compounds lacking OH, NH, and other hydrogen-bonding functional groups.

We showed earlier that reactions of NaCp and hexafluorobenzene afford pentafluorophenyl-substituted cyclopentadienes, which we used in a general synthesis of C_6F_5-substituted metallocene complexes.[11] It seemed reasonable that 1,1-dilithioferrocene (**1**)[12] would react with fluoroaromatic compounds such as hexafluorobenzene (Scheme 1) to give fluoroarylated ferrocenes more directly. We sought to prepare a variety of fluoroarylated ferrocene complexes by this route as part of our ongoing investigation of the effects of fluoroaryl substituents on the structure, physical and spectroscopic properties, and reactivity of metallocenes and other Cp complexes.

In our initial experiment, we used only a small excess of C_6F_6, and in addition to the desired diarylated ferrocene (**2**), a complex mixture of dark orange-red, poorly soluble byproducts was obtained (Scheme 1). Preliminary analyses of the byproduct mixture suggested the presence of linear, alternating 1,1′-ferrocenylene−1,4-tetrafluorophenylene co-oligomers (**4**). This paper presents our attempts to optimize the formation of these oligomeric, or polymeric, species (**4**). Ultimately, the low solubility of **4** as well as insurmountable difficulties in the purification and characterization of the lithioferrocene intermediates frustrated our efforts to obtain high polymers by this step-growth process.[13] However, in the course of these studies, we isolated several arylated ferrocenes and diferrocenylarene complexes, and we found that these complexes show several interesting and pervasive solid-state structural motifs, including intramolecular (transannular) arene stacking, intermolecular arene−Cp stacking, and networks of C−H···F−C interactions. This contribution presents the syntheses of these new complexes and an analysis of the trends in their structural data.

Results and Discussion

Synthesis of Monometallic Complexes. Dilithioferrocene reacted with an excess of C_6F_6 to produce the diarylated ferrocene (**2**) as the major product. We prepared complex **2** previously by the reaction of $FeBr_2$ with $Na(C_6F_5Cp)$.[11] Among the byproducts of this reaction were species that had NMR spectra tentatively assigned to structural motifs (**A** and **B**) in which either *n*-butyllithium or 1,2-bis(dimethylamino)ethyllithium displaced aromatic fluorides of C_6F_6 or of the product **2**. Momentary isolation and washing of the dilithioferrocene intermediate **1** minimized the formation of these byproducts in subsequent reactions with C_6F_6. We found that **1** is not sufficiently stable for long-term storage (even in our glovebox freezer at −35 °C). Also, the ^{1}H NMR spectra of **1** showed varying amounts of residual *N*,*N*,*N*′,*N*′-tetramethylethylenediamine (TMEDA) as well as broad spectral features attributed to aggregation processes. The presence of monolithioferrocene could be neither confirmed nor ruled out by spectroscopic means.

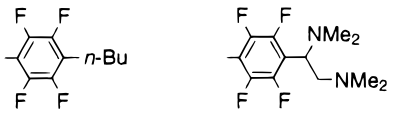

We next attempted to generalize the route shown in Scheme 1 to substituted ferrocenes. Treatement of 1,1′-dimethylferrocene or 1,1′-bis(trimethylsilyl)ferrocene using n-BuLi/TMEDA in hexanes followed by electrophilic quenching (Me_3SiCl) and subsequent ^{1}H NMR analysis of the product mixture showed that lithiation was incomplete even after long reaction times with large excesses of n-BuLi. However, the commercially available tertiary amine **5** was previously known to undergo highly efficient and regioselective lithiation with 1 or 2 equiv of n-BuLi/TMEDA (Scheme 2) to afford the monolithiated (**6**) or dilithiated (**9**) intermediates, respectively.[14] Subsequent reactions of **6** or **9** with excess hexafluorobenzene afforded the corresponding arylated ferrocenes (**7** and **10**, respectively) in moderate yields.

(5) Hollandsworth, C. B.; Hollis, W. G., Jr.; Slebodnick, C.; Deck, P. A. *Organometallics* **1999**, *18*, 3610.
(6) (a) Nangia, A.; Desiraju G. R. *Top. Curr. Chem.* **1998**, *198*, 57. (b) Aakeroy, C. B.; Borovik, A. S. *Coord. Chem. Rev.* **1999**, *183*, 1.
(7) (a) Braga, D.; Grepioni, F. *Coord. Chem. Rev.* **1999**, *183*, 19. (b) Rivas, J. C. M.; Brammer, L. *Coord. Chem. Rev.* **1999**, *183*, 43.
(8) (a) Renak, M. L.; Bartholomew, G. P.; Wang, S. J.; Ricatto, P. J.; Lachicotte, R. J.; Bazan, G. C. *J. Am. Chem. Soc.* **1999**, *121*, 7787. (b) Row: T. N. G. *Coord. Chem. Rev.* **1999**, *183*, 81. (c) Evans, T. A.; Seddon, K. R. *Chem. Commun.* **1997**, 2024. (d) Williams, J. H.; Cockcroft, J. K.; Fitch, A. N. *Angew. Chem., Int. Ed. Engl.* **1992**, *31*, 1655.
(9) Weck, M.; Dunn, A. R.; Matsumoto, K.; Coates, G. W.; Lobkovsky, E. B.; Grubbs, R. H. *Angew. Chem., Int. Ed.* **1999**, *38*, 2741.
(10) Thalladi, V. R.; Weiss, H.-C.; Bläser, D.; Boese, R.; Nangia, A.; Desiraju, G. R. *J. Am. Chem. Soc.* **1998**, *120*, 8702.
(11) Deck, P. A.; Jackson, W. F.; Fronczek, F. R. *Organometallics* **1996**, *15*, 5287−5291.
(12) (a) Guillaneux, D.; Kagan, H. B. *J. Org. Chem.* **1995**, *60*, 2502. (b) Riant, O.; Argouarch, G.; Guillaneux, D.; Samuel, O.; Kagan, H. B. *J. Org. Chem.* **1998**, *63*, 3511. (c) Dietz, S. D.; Bell, W. L.; Cook, R. L. *J. Organomet. Chem.* **1997**, *546*, 67. (d) Rausch, M. D.; Moser, G. A.; Meade, C. F. *J. Organomet. Chem.* **1973**, *51*, 1. (e) Slocum, D. W.; Englemann, T. R.; Ernst, C.; Jennings, C. A.; Jones, W.; Koonsvitsky, B.; Lewis, J.; Shenkin, P. *J. Chem. Educ.* **1969**, *46*, 145.

(13) In step-growth polymerization, a fractional monomer impurity (p) leads to a limit in the number-averaged degree of oligomerization according to the Carothers equation, $D = (1 - p)^{-1}$. See: Flory, P. J. *Principles of Polymer Chemistry*; Cornell University Press: Ithaca, 1953; p 81.

Scheme 2

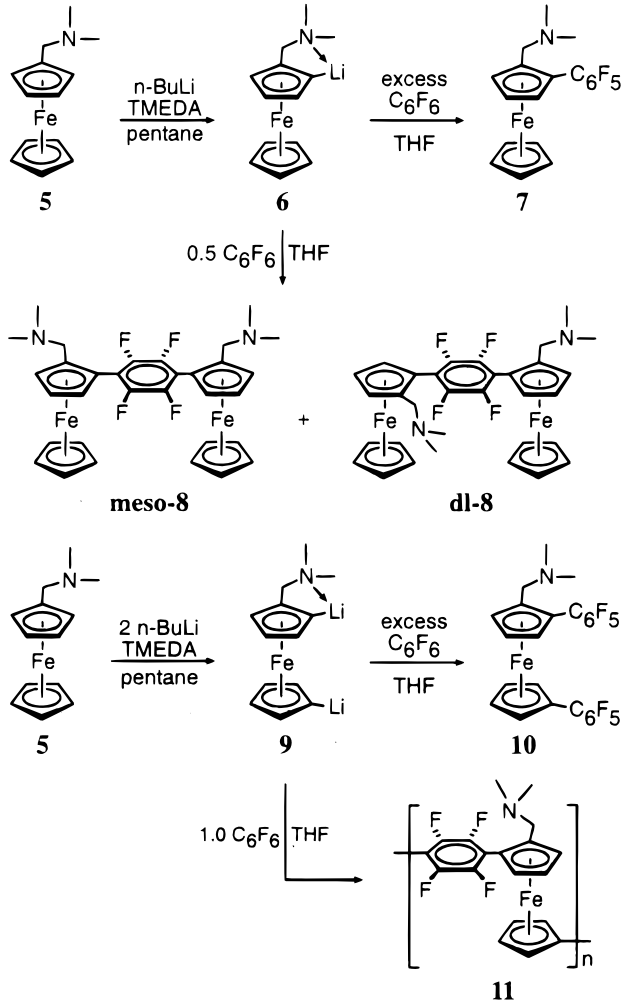

Conformational rotation about the C_6F_5−Cp axis in these compounds is relatively free. For example, using ^{19}F NMR analysis, the diastereotopic ortho C−F signals in **7** showed a coalescence temperature of about −60(5) °C in CD_2Cl_2, and the corresponding ortho C−F signals of **10** (for C_6F_5 attached to R^NCp) and of **2** were still in pseudo-fast exchange at −75 °C.

Isolation and Characterization of Dimetallic Complexes. As shown in Scheme 1, the reaction of $(LiCp)_2Fe$ and C_6F_6 (1:1 ratio) afforded a mixture of oligomeric species. The shortest "oligomer", the diiron complex **3**, was isolated from the product mixture and characterized. The ^{19}F NMR spectrum of **3** was instructive. A sharp singlet (4 F) for the bridging 1,4-C_6F_4 group confirmed the regioselectivity of aromatic substitution in the "repeat unit", whereas three additional signals (total of 10 F) indicated two chemically equivalent C_6F_5 "end groups". The crystal structure and the solution voltammetric analysis of **3** are discussed below.

The reaction of the monolithiated intermediate **6** with C_6F_6 (2:1 ratio) afforded the diiron complex **8** as a mixture of meso and dl diastereomers (Scheme 2). The ^{19}F NMR spectrum of this mixture showed that the ratio of ***meso*-8** to ***dl*-8** was about 3:2, determined by comparing the relative intensities of the two singlets at −138.80 ppm (***meso*-8**) and −138.65 ppm (***dl*-8**) in $CDCl_3$. Miraculously, ***meso*-8** and ***dl*-8** were separated simply by repeated extraction of the mixture with hexanes at 25 °C until the filtrate ran colorless to the eye. The filter cake was 95% pure ***meso*-8**, and the complex isolated from the filtrate was 97% pure ***dl*-8**, as determined by ^{19}F NMR analysis. The relative configuration of ***meso*-8** was confirmed by obtaining a crystal structure of the corresponding bis(methiodide) derivative (see below). These compounds are reminiscent of the "planar-chiral" ferrocenes that have attracted attention as ligands for stereoselective catalysts.[15] Work is underway to resolve ***dl*-8** by fractional crystallization of the bis(hydrocamphorsulfonate).

Isolation and Characterization of Oligomeric Species. Our initial plan of isolating alternating ferrocenylene−tetrafluorophenylene copolymers met with varied results. We conjectured that the diiron complex **3** was produced by a step-growth process (Scheme 1) and should be accompanied by linear, oligomeric homologues (**4**). Unfortunately, the product mixture **4** was not soluble enough (e.g., in ether, dichloromethane, chloroform, benzene, or ethyl acetate) for chromatographic separations or fractional crystallization. Despite the presence of perfluoroaromatic groups, the solubility of **4** was not noticeably improved in "fluorous" solvents[16] such as hexafluorobenzene or 1-(perfluorobutyl)tetrahydrofuran. We used Soxhlet extraction of crude **4** with a series of solvents having increasing boiling points (benzene, toluene, chlorobenzene, and 1,2-dichlorobenzene) to separate **4** into several "extracts". Analysis of the initial benzene "extract" showed the same general spectroscopic features as **3** (internal 1,4-C_6F_4 and end group C_6F_5, both considerably broadened), but with much lower relative integration of the end groups. The ^{1}H NMR spectrum also showed a low population of unsubstituted Cp end groups. We estimated the number-averaged degree of oligomerization to be in the range $10 < D_n < 20$. End group analysis alone cannot rule out macrocyclic species. Moreover, the "extract" was only partially dissolved in the NMR solvent ($CDCl_3$), so the solid substance was not sampled representatively. Triiron, tetrairon, and pentairon homologues of **3** were detected as a progression of signals separated by about 330 amu in their mass spectra (EI, positive ion). The repeat unit of the oligomer has a mass of 332 amu. In contrast to our recent report of octafluorobiphenylene-linked oligoferrocenes,[5] the triiron and tetrairon oligomers of **4** could not be separated chromatographically on either silica gel or alumina. Surprisingly, direct probe CI (positive and negative ion), FAB, and MALDI-TOF mass spectrometric techniques all failed to give useful spectra.[17] The "extracts" obtained using toluene, chlo-

(14) (a) Xiao, L.; Mereiter, K.; Weissensteiner, W.; Widhalm, M. *Synthesis* **1999**, *8*, 1354. (b) Hitchcock, P. B.; Hughes, D. L.; Leigh, G. J.; Sanders, J. R.; De Souza, J. S. *J. Chem. Soc., Dalton Trans.* **1999**, *7*, 1161. (c) Nishibayashi, Y.; Yasuyoshi, A.; Ohe, K.; Uemura, S. *J. Org. Chem.* **1996**, *61*, 1172. (d) Slocum, D. W.; Jennings, C. A.; Engelmann, T. R.; Rockett, B. W.; Hauser, C. R. *J. Org. Chem.* **1971**, *36*, 377. (e) Marr, G. *J. Organomet. Chem.* **1967**, *9*, 147.

(15) (a) Houdus, B. L.; Ruble, J. C.; Fu, G. C. *J. Am. Chem. Soc.* **1999**, *121*, 2637−2638. (b) Widhalm, M.; Mereiter, K.; Bourghida, M. *Tetrahedron: Asymmetry* **1998**, *9*, 2983. (c) Riant, O.; Samuel, O.; Flessner, T.; Taudien, S.; Kagan, H. B. *J. Org. Chem.* **1997**, *62*, 6733.

(16) (a) Fish, R. H.; *Chem. Eur. J.* **1999**, *5*, 1677. (b) Juliette, J. J. J.; Rutherford, D.; Horvath, I. T.; Gladysz, J. A. *J. Am. Chem. Soc.* **1999**, *121*, 2696. (c) Smith, D. C.; Stevens, E. D.; Nolan, S. P. *Inorg. Chem.* **1999**, *38*, 5277. (d) Barthel-Rosa, L. P.; Gladysz, J. A. *Coord. Chem. Rev.* **1999**, *192*, 587. (e) de Wolf, E.; van Koten, G.; Deelman, B. J. *Chem. Soc. Rev.* **1999**, *28*, 37. (f) Horvath, I. T. *Acc. Chem. Res.* **1998**, *31*, 641.

Table 1. Crystallographic Data

	3	**7**	**10**	**12**·3CHCl$_3$
empirical formula	$C_{38}H_{16}F_{14}Fe_2$	$C_{19}H_{16}F_5FeN$	$C_{25}H_{15}F_{10}FeN$	$C_{37}H_{41}Cl_9F_4Fe_2I_2N_2$
fw	850.21	409.18	575.23	1274.27
diffractometer	Siemens P4	Siemens P4	Siemens P4	Enraf-Nonius CAD4
cryst dimens (mm)	0.1 × 0.2 × 0.08	0.28 × 0.34 × 0.41	0.5 × 0.5 × 0.1	0.50 × 0.40 × 0.37
cryst syst	monoclinic	monoclinic	monoclinic	monoclinic
a (Å)	11.330(3)	17.0820(11)	7.1150(10)	12.897(1)
b (Å)	6.565(2)	6.7453(5)	32.954(3)	27.419(3)
c (Å)	20.192(5)	15.8893(10)	10.1340(10)	14.091(3)
β (deg)	94.04(3)	111.234(5)	104.640(10)	110.29(1)
V (Å)^3	1498.2(8)	1706.5(2)	2299.0(4)	4673(1)
space group	$P2(1)/c$	$P2(1)/c$	$P2(1)/c$	$C2/m$
Z	2	4	4	4
D_{calc} (Mg m^{-3})	1.885	1.593	1.662	1.760
abs coeff (mm^{-1})	1.088	0.937	0.752	2.490
F_{000}	844	832	1152	2428
λ(Mo Kα) (Å)	0.71073	0.71073	0.71073	0.71073
temp (K)	298(2)	298(2)	293(2)	100(2)
θ collection range	1.80−25.01	2.56−25.00	2.17−25.00	2.75−29.98
no. of reflns colld	3641	3937	5203	7188
no. of indep reflns	2640	2994	4010	6938
abs corr method	integration	integration	ψ scans	ψ scans
max, min transm	0.8414, 0.8030	0.7828, 0.6767	0.8929, 0.7085	0.398, 0.328
no. of data/restrs/params	2399/0/245	2994/0/299	3639/0/335	6938/0/260
R [$I > 2\sigma(I)$]	0.0506	0.0316	0.0511	0.0387
R_w [$I > 2\sigma(I)$]	0.1273	0.0686	0.1306	0.1023
GoF on F^2	1.015	0.876	1.071	1.051
diff peak, hole (e Å^{-3})	0.782, −0.685	0.201, −0.287	0.37, −0.414	3.043, −1.722

robenzene, and dichlorobenzene yielded only intractable red to red-brown solids.

The reaction of the *substituted* dilithiated ferrocene derivative **9** with 1 equiv of C_6F_6 (Scheme 2) afforded an orange-red solid (**11**) that was freely soluble in benzene, dichloromethane, chloroform, and ether, but only partly soluble in hexanes and methanol. Crude **11** was purified by chromatography on alumina mainly to remove small amounts of mononuclear complexes such as **7** and **10**. The isolation of the monoarylated complex **7** suggested that the dilithiated intermediate **9** either contained some **6** or had abstracted protons from the solvent, neither of which can be tolerated in the synthesis of a high polymer. ^{1}H and ^{19}F NMR spectra of the "purified" oligomer **11** were consistent with the assigned structure. Using mononuclear complexes **7** and **10** as models for chemical shift assignments, the number-average degree of polymerization (n) of **11** was estimated to be approximately 9 ± 1, corresponding to a molecular weight (M_n) of 3500 ± 500. Details of this "end group" analysis (spectral assignments and algebraic workup of integration data) are provided in the Supporting Information. Published step-growth routes to ferrocene-containing polymers gave similar degrees of oligomerization.[4]

Crystallographic Analyses. Collection and refinement data for the X-ray diffraction analysis of **3**, **7**, **10**, and **12** are compiled in Table 1. Complete tables of crystallographic data are deposited in the Supporting Information.

The structure of **7** (Figure 1) is highly regular, with no significant difference between the two Fe−Cp(centroid) distances (1.651 and 1.659 Å) and a Cp(centroid)−Fe−Cp(centroid) angle of 177.6°. The dimethylaminomethyl substituent adopts a conformation (N−CH$_2$−C(2)−C(1) = −123.7°) in which the non-bonding pair of

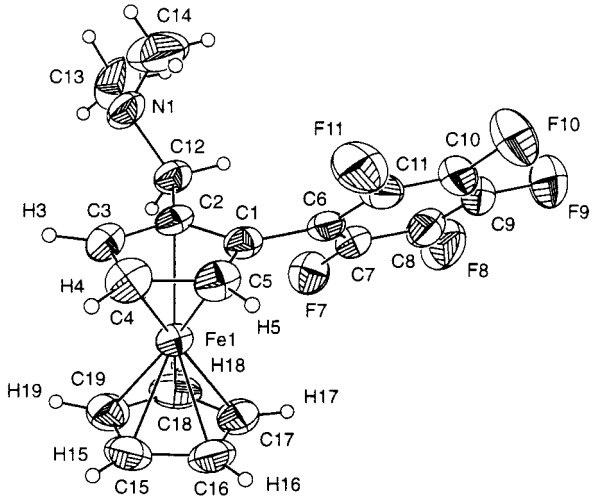

Figure 1. Thermal ellipsoid plot of **7** shown at 50% probability.

electrons on nitrogen is directed away from the C_6F_5 substituent (compare **10**, below). The Cp−C_6F_5 torsion angle is 48.4°.

The ferrocene moiety of **10** (Figure 2) is relatively undistorted, with equal Fe−Cp(centroid) distances (1.653 and 1.645 Å), parallel Cp ligands (2.9° interplanar angle), and Fe−C distances within 0.027 Å of their mean. The two ipso carbons, C(14) and C(20), of the C_6F_5 groups appear slightly bent out of the C_5 least-squares planes of the Cp ligands, away from the iron atom, by 0.027 and 0.032 Å, respectively. Fluorine atom positions deviated no more than 0.051 Å from their respective C_6 least-squares planes. The Cp−C_6F_5 interplanar torsion angles were 40.7° and 32.4°. The dimethylaminomethyl substituent of **10** adopts a conformation (N−CH$_2$−C(2)−C(1) = −54.5°) in which the pair of nitrogen nonbonding electrons is directed toward the center of the C_6F_5 group attached to the same Cp ligand (compare **7**, above). The lack of a clear trend in the disposition of the CH$_2$N(CH$_3$)$_2$ group suggests that this substituent will not

(17) For a discussion of MALDI applications in oligoferrocene characterization, see: Juhasz, P.; Costello, C. E. *Rapid Commun. Mass Spectrom.* **1993**, *7*, 343.

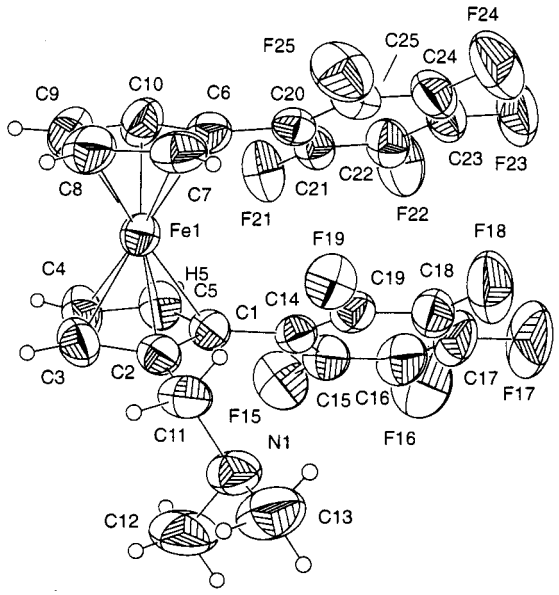

Figure 2. Thermal ellipsoid plot of **10** shown at 50% probability.

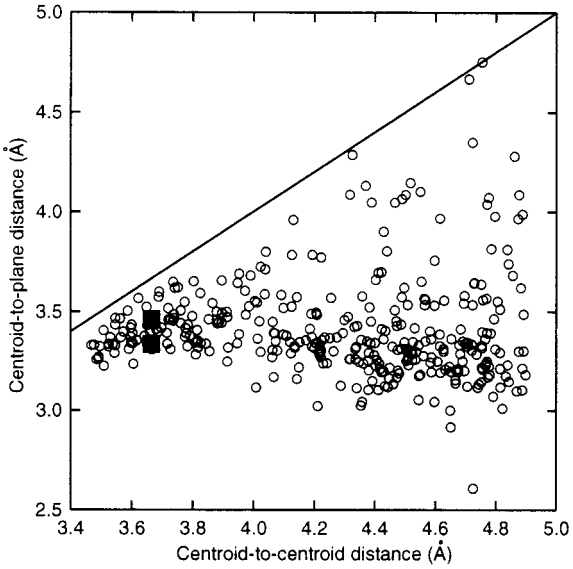

Figure 3. Scatterplot of parameters for $C_6F_5-C_6F_5$ arene stacking interactions from the Cambridge Crystallographic Database. All interactions having centroid−centroid distances less than 4.9 Å were included.

serve as reliable design element for ordered solids without the directing effects of hydrogen bond donors.

Further inspection of the structure of **10** reveals intramolecular stacking of the two C_6F_5 groups characterized by an interplanar (C_6-C_6) angle of 10.1°, a centroid-to-centroid distance of 3.66 Å, and two centroid-to-plane distances of 3.33 and 3.46 Å. We infer that a "purposeful" stacking interaction is the reason for the eclipsed Cp−Fe−Cp conformation observed in **10**. To better characterize this stacking interaction, we compared the $C_6F_5-C_6F_5$ centroid−centroid distances with data obtained from the Cambridge Crystallographic Database (364 structures displayed $C_6F_5-C_6F_5$ centroid−centroid distances less than 4.9 Å). The results are shown in Figure 3 (darkened squares represent data from **10**). The line drawn in Figure 3 represents an "idealized" stacking arrangement in which the vector connecting the two centroids is perpendicular to both

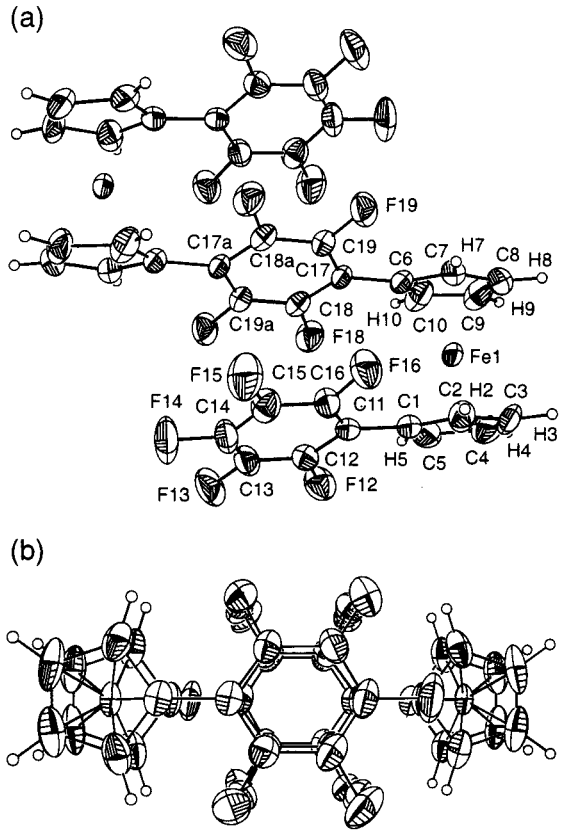

Figure 4. Thermal ellipsoid plot of **3** shown at 50% probability.

C_6 planes. Note that no points may appear above this "boundary" line, because a centroid−centroid distance must be at least as long as the corresponding centroid−plane distance. As centroid−centroid distances become shorter, interactions among the anisotropic charge distributions responsible for stacking become stronger, and alignment of the C_6F_5 groups increasingly adheres to an empirical "rule" defined by the clustering of points toward the left of Figure 3. Note that this "rule" does *not* enforce the "idealized" (coplanar, cofacial) geometry represented by the boundary line. We describe the stacking interaction in **10** as "purposeful", because its location among the points clustered toward the left of Figure 3 suggest that it follows the "rule".

In the crystalline lattice of the diiron complex **3**, each molecule is situated on a crystallographic inversion center, so that half of the molecule defines the asymmetric unit. The complex adopts an S-shaped conformation (Figure 4a), in which the three fluoroaryl groups are stacked nearly parallel to one another (Figure 4b). The interaction is defined by a $C_6F_5-C_6F_4$ interplanar (C_6-C_6) angle of 5.8°, a C_6(centroid)−C_6(centroid) distance of 3.671 Å, and two centroid-to-plane distances of 3.383 and 3.366 Å, nearly identical to the corresponding parameters in **10**, again suggesting a "purposeful" intramolecular arene stacking interaction. The Cp−C_6F_5 and Cp−C_6F_4 torsion angles (21.4° and 23.6°, respectively) are relatively shallow compared to the corresponding parameters in **7** and **10** (see above). The ipso carbons, C(11) and C(17), of the C_6 rings are bent slightly out of the C_5 least-squares planes of the Cp ligands, away from the iron atom, by 0.027 and 0.032 Å, respectively. Otherwise, the ferrocene portion of the

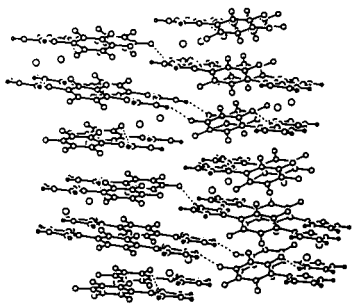

Figure 5. Stereoview of packing diagram of **3**.

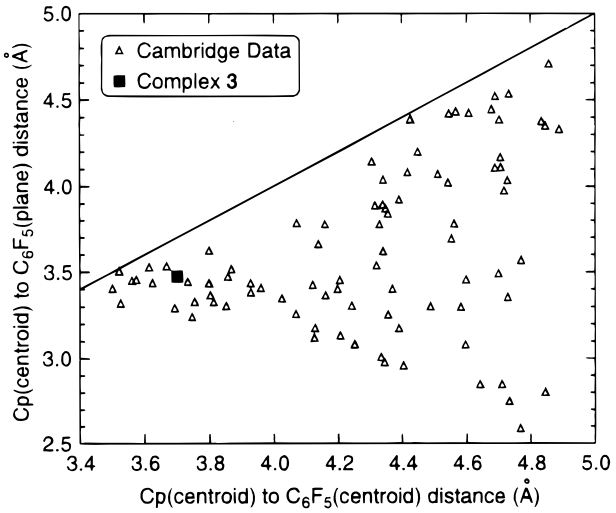

Figure 6. Scatterplot of parameters for Cp−C_6F_5 π-stacking interactions from the Cambridge Crystallographic Database. All interactions having centroid−centroid distances less than 4.9 Å were included.

asymmetric unit exhibits a relatively undistored structure, with Fe−Cp(centroid) distances of 1.641 and 1.648 Å, parallel Cp ligands (3.9° interplanar angle), and uniform Fe−C distances (within 0.012 Å of their mean). The pentafluorophenyl group is planar (mean deviation of 0.006 Å from the C_6 least-squares plane), as is the central tetrafluorophenylene group (mean deviation of 0.002 Å from the least-squares plane).

The packing diagram of **3** (Figure 5) reveals further stacking interactions of aromatic groups in the crystalline lattice. The two Cp ligands of each ferrocene group alternate with the three fluoroaryl groups of a neighboring molecule in nearly linear, infinite stacking chains. This result contrasts both the structure of **10**, in which the dimethylaminomethyl group appears to impede analogous stacking, and the structure of 1,1′-metallocenylene-1,8-naphthalenylene co-oligomers,[18] which showed only Cp−Cp stacking. The intermolecular Cp(centroid)−C_6F_5(centroid) distance in **3** is 3.707 Å, while the Cp(centroid)−C_6F_5(least-squares plane) distance is 3.474 Å. The Cp and C_6F_5 least-squares planes intersect in a 21.4° angle. These data are placed into the context of 90 other Cp−C_6F_5 interactions (centroid−centroid distance less than 4.9 Å) extracted from the Cambridge Crystallographic Data Centre (Figure 6). In accordance with the discussion of C_6F_5−C_6F_5 interactions in **10** (above), the decreased scatter toward the left of Figure 6 reflects increasingly well-defined interactions at closer Cp−C_6F_5 distances. Thus, the position of the filled square (representing **3**) in this portion of the scatterplot suggests a "purposeful" Cp−C_6F_5 contact in crystalline **3**.

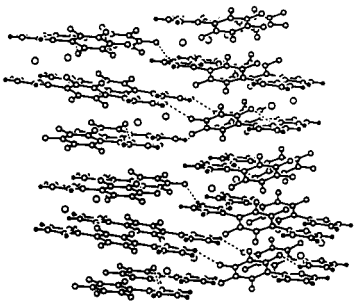

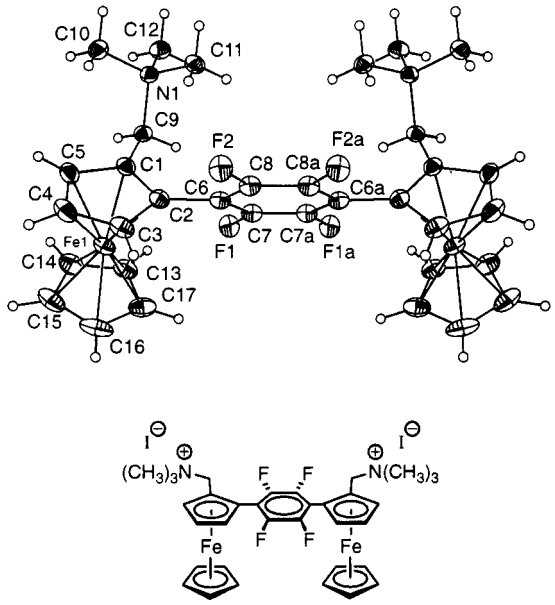

meso-12

Figure 7. Thermal ellipsoid plot of the dicationic portion of ***meso*-12** shown at 50% probability.

The structure of **12** is shown in Figure 7. Our objective was to assign the structure of the corresponding free base (***meso*-8**), which did not form useful single crystals from several solvent combinations that we tried. The molecule **12** rests on a crystallographic mirror plane, with half of the molecule as the asymmetric unit. The structure has disordered lattice solvent molecules (chloroform and perhaps water; please see the Experimental Section), which did not interfere with relatively precise estimation of bond lengths and angles in the molecular structure of the dimetallic dication. One iodide ion, I(1), rests on a 2-fold position, while I(2) and I(3) rest on 2/m positions. Noteworthy are the conformational disposition of the trimethylammoniomethyl substituent (N−CH_2−C(1)−C(2) = −96.0°) directing the nitrogen anti to the iron atom, possibly to minimize partial charge repulsions. The large Cp−C_6F_4 interplanar torsion angle (54.8°) avoids steric interactions between the fluorine atoms and the trimethylammonio group. The metallocene structure is relatively undistorted, with average deviations from the C(1)−C(2)−C(3)−C(4)−C(5) and the C(13)−C(14)−C(15)−C(16)−C(17) planes of 0.003 and

(18) Hudson, R. D. A.; Foxman, B. M.; Rosenblum, M. *Organometallics* **1999**, *18*, 4098.

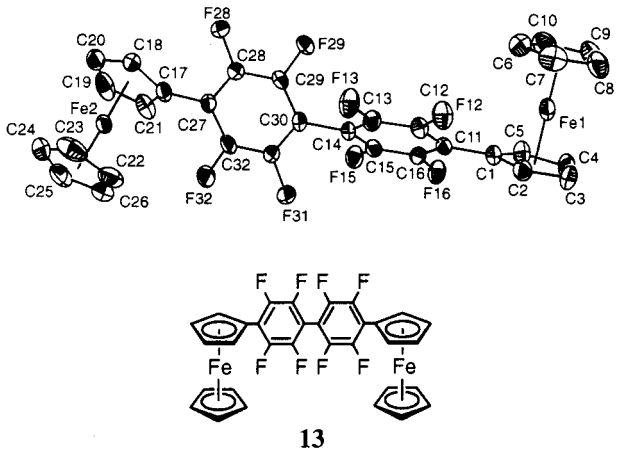

13

Figure 8. Structure of **13**. (a) Numbering scheme with hydrogen atoms removed for clarity. Hydrogen atoms are numbered the same as the carbon atoms to which they are attached. (b) Packing diagram showing intermolecular C−H···F−C interactions.

0.002 Å, respectively. The interplanar angle of the two Cp ligands is 3.5°. The displacement of the C_6F_4 ipso carbon from the attached Cp plane is 0.142 Å in the direction distal to iron as in **7** and **10**, above, but greater in magnitude. This results in a "wishbone" distortion in which the unsubstituted Cp ligands are pulled apart from one another. The angle between the least-squares Cp planes C(1)−C(2)−C(3)−C(4)−C(5) and C(1A)−C(2A)−C(3A)−C(4A)−C(5A) is 14.5°.

Inter- and intramolecular C−H···F interactions are prevasive in the crystal structures of **3**, **7**, **10**, **12**, and **13**. The synthesis and crystallographic characterization of complex **13** are reported elsewhere;[5] please refer to the numbering scheme in Figure 8. Several investigators have addressed the issue of whether such C−H···F interactions should be considered "hydrogen bonds".[19] Dunitz and Taylor[19b] suggested that an H···F distance less than 2.3 Å is an appropriate criterion for hydrogen bonding, because the sum of the van der Waals radii of hydrogen and fluorine is in the range 2.5−2.7 Å[20] and because H···N and H···O hydrogen bonds generally exhibit H···X distances that are significantly shorter than the sum of their respective van der Waals radii. They concluded that C−F bonds are poor hydrogen-bond acceptors and that donors such as O−H, N−H, and C−H will interact with stronger acceptors if available. In general, interactions among organic C−F and C−H groups must often coexist with various other intermolecular packing motifs, which leads to a broad range of observed H···F distances and C−H···F angles.[10] In the absence of stronger acceptors, however, "close" C−H···F−C contacts are relatively common: 39 compounds having H···F distances of less than 2.35 Å were found among 360 compounds in the Cambridge Crystallographic Database containing sp^2-hybridized C−F bonds.[21] Desiraju and co-workers[10] advanced the alternative criterion of a strict, inverse correlation between

Table 2. Unique Intermolecular C−H···F−C Interactions in the Crystal Structures of 3, 7, 10, 12, and 13

compound	interaction	H···F (Å)	C−H···F (deg)
3	C3−H3···F13	2.84	117.1
	C4−H4···F13	2.99	111.5
	C5−H5···F16	2.55	153.2
	C8−H8···F15	2.97	174.1
	C8−H8···F19	2.99	113.8
	C9−H9···F14	2.48	156.4
7	C5−H5···F7	2.58	149.5
10	C3−H3···F22	2.89	137.9
	C4−H4···*F*23	2.56	148.3
	C5−H5···F19	2.60	152.5
	C8−H8···F22	2.59	144.7
	C8−H8···*F*23	2.75	140.7
	C9−H9···F25	2.70	144.6
	C10−H10···F24	2.57	115.0
	C10−H10···F19	2.60	151.7
12	C3−H3···F2	2.89	148.5
13	C2−H2···F28	2.88	153.3
	C3−H3···F13	2.64	146.7
	C3−H3···F29	2.96	141.5
	C8−H8···F13	2.77	145.4
	C9−H9···F16	2.73	165.6
	C18−H18···F15	2.72	139.1
	C18−H18···F29	2.85	102.3
	C18−H13···F31	2.95	161.0
	C20−H20···F16	2.97	110.3
	C21−H21···F12	2.49	146.7
	C23−H23···F12	2.77	136.9
	C25−H25···F16	2.75	152.6
	C26−H26···F28	2.72	174.0

H···F distances and C−H···F angles. However, their study was limited to a very narrow range of compounds (fluorinated benzenes), wherein rigid structure, high molecular symmetry, relatively constant molecular "shape", and a lack of other competing structural influences (such as *intra*molecular C−H···F interactions) contribute to a much cleaner correlation among selected metric parameters. They concluded that *only* compounds consisting of C, H, and F atoms are "appropriate" for the study of C−H···F interactions and that the C−H groups must be "acidic". The latter criterion is ostensibly satisfied in ferrocenes, which have relatively acidic Cp C−H bonds, evidenced by their facile metalation. We assert that the presence of coordinatively saturated iron atoms embedded in complexes such as **3** or **13** should not make these species "inappropriate" for the study of C−H···F interactions.

H···F distances and C−H···F angles for complexes **3**, **7**, **10**, **12**, and **13** are listed in Table 2 and presented in a scatterplot (Figure 9). The small, unfilled circles (Figure 9) represent the data of Desiraju and co-workers for fluorinated benzenes.[10] Indeed, their data show an impressive inverse correlation with very little scatter. This correlation can be considered a "rule" for C−H···F−C interactions. Next, consider the data for complex **3** (filled circles in Figure 9), which follows the same trend except for a single interaction in the upper right quadrant of the scatterplot. We infer that the C−H···F−C interactions in **3** (dotted lines in Figure 5) represent "purposeful" interactions in the sense that they follow the "rule" established by the fluorinated benzenes, with *one* additional, "diffuse" C−H···F−C interaction accompanying the otherwise optimal packing arrangement. In contrast, the packing in complex **13** is dominated by a large number of "diffuse" interactions, represented by highly scattered squares in the upper

(19) (a) Grepioni, F.; Cojazzi, G.; Draper, S. M.; Scully, N.; Braga, D. *Organometallics* **1988**, *7*, 296. (b) Dunitz, J.; Taylor, R. *Chem. Eur. J.* **1997**, *3*, 89. (c) Plenio, H. *Chem. Rev.* **1997**, *97*, 3363.

(20) (a) Bondi, A. *J. Phys. Chem.* **1964**, *68*, 441. (b) Rowland, R. S.; Taylor, R. *J. Phys. Chem.* **1996**, *100*, 7384.

(21) Howard, J. A. K.; Hoy, V. J.; O'Hagan, D.; Smith, G. T. *Tetrahedron* **1996**, *52*, 12613.

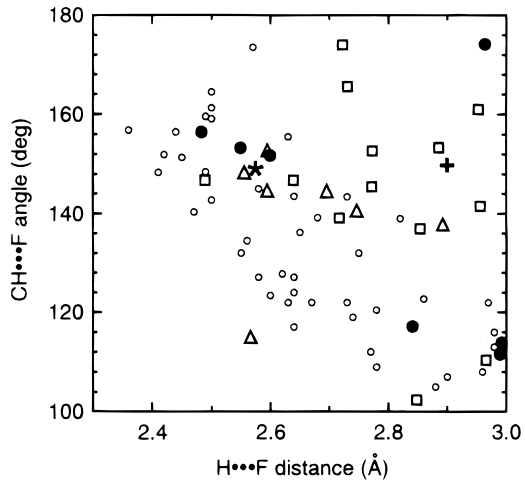

Figure 9. Scatterplot of H···F and C−H···F angles: (●) data for **3**; (∗) data for **7**; (△) data for **10**; (□) data for **13**; (○) data for fluorinated benzenes from ref 10.

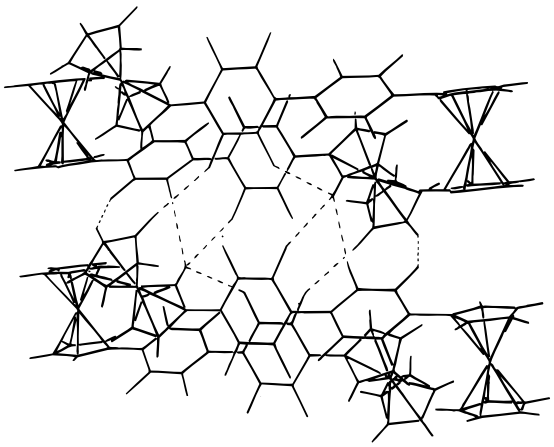

Figure 10. Packing diagram of **13** showing intermolecular C−H···F−C interactions as dotted lines.

right quadrant of Figure 9. The lack of specific, "purposeful" H···F contacts in **13** is also reflected in the extensive, unsymmetrical bifurcation of these interactions, as illustrated in Figure 10. Next, consider the data for complex **10** (triangles in Figure 9), which shows a weak distance−angle correlation, excluding the single point in the lower left quadrant. We propose that the six weaker C−H···F−C interactions and the irregular shape of the molecule constrain the last C−H···F−C interaction into an "awkward" geometry in order to optimize the overall packing arrangement. The monoarylated complex **7** exhibited only one C−H···F−C interaction less than 3.0 Å (asterisk in Figure 9), while the single C−H···F−C interaction in **12** exhibited two, symmetry-related interactions (dotted lines in Figure 11, plus symbol in Figure 9). It should be noted that the closest N···H contacts in **7** are 2.87 and 3.02 Å, while there are no N···H interactions evident in **10**, suggesting that F−C acceptors compete effectively with the nitrogen acceptors for C−H donors in these compounds.

Considering the relatively narrow range of C_6F_5−Cp torsion angles in our compounds (see above), it is not surprising that the metric data for *intra*molecular C−H···F−C interactions (Table 3) are also narrowly distributed. Figure 12 illustrates these intramolecular C−H···F−C contacts. Two polymorphs of 2,3,4,5,6-pentafluorobiphenyl have been characterized crystallographically,[22] and these show analogous ortho−ortho H···F distances of 2.68 and 2.80 Å, similar to the values shown in Table 3.

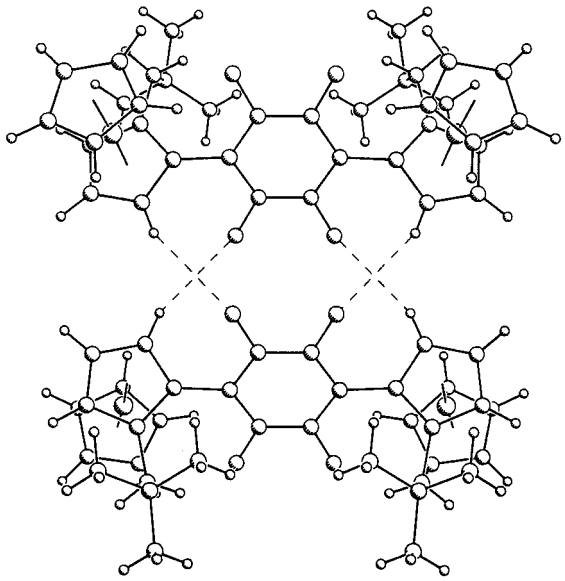

Figure 11. Packing diagram of **12** (dication) showing intermolecular C−H···F−C interactions as dotted lines.

Table 3. Unique Intramolecular C−H···F−C Interactions in the Crystal Structures of 3, 7, 10, 12, and 13

compound	interaction	H···F (Å)	C−H···F (deg)
3	C2−H2···F16	2.37	108.2
	C5−H5···F12	2.33	108.3
	C7−H7···F19	2.38	106.9
	C10−H10···F18	2.38	107.4
7	C5−H5···F11	2.74	92.2
	C17−H17···F7	2.63	109.0
10	C5−H5···F21	2.61	114.3
	C5−H5···F15	2.53	97.9
	C7−H7···F19	2.72	108.7
	C7−H7···F25	2.52	101.8
	C10−H10···F21	2.49	103.9
12	C3−H3···F2	2.87	86.3
	C13−H13···F1	2.62	104.3
	C17−H17···F1	2.72	100.7
13	C2−H2···F12	2.55	104.8
	C5−H5···F16	2.53	100.6
	C6−H6···F12	2.87	111.1
	C18−H18···F32	2.67	106.0
	C21−H21···F28	2.59	98.6
	C26−H26···F32	2.75	110.9

Electrochemical Analysis of 3. Cyclic voltammetric analysis of **3** showed a single, reversible oxidation/reduction wave having an $E_{1/2}$ of 340(10) mV relative to $Fc^+|Fc$ in dichloromethane. The Osteryoung square wave voltammogram (Figure 13) showed a slightly broadened signal (fwhm = 132 mV), indicating a small, unresolved splitting of two $Fe^{III}|Fe^{II}$ couples. The difference in line widths between the diiron complex (**3**, fwhm = 132 mV) and the internal standard (ferrocene, fwhm = 106) suggests a difference of only about 26(10) mV between the first and second oxidations of **3**, which would then be characterized by $E_{1/2}$ values of 323(10) and 349(10) mV. These oxidation potentials are close to the value of 345(5) mV observed for $(C_6F_5Cp)_2Fe$,[11]

(22) Brock, C. P.; Naae, D. G.; Goodhand, N.; Hamor, T. A. *Acta Crystallogr. B* **1978**, *34*, 3691.

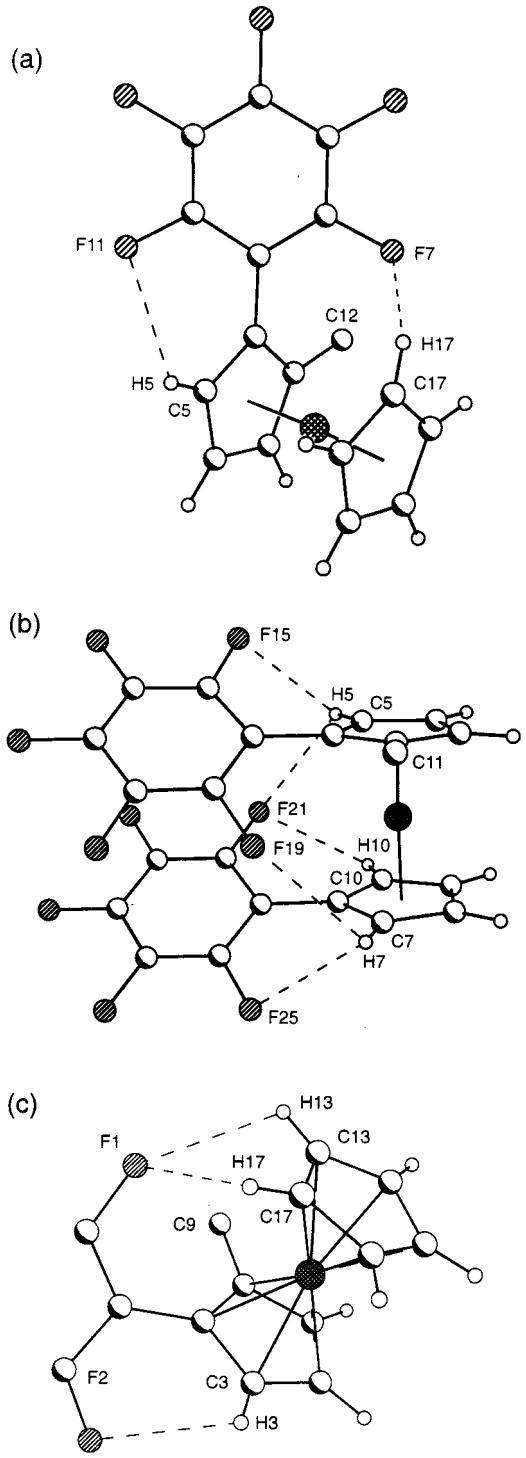

Figure 12. Diagrams showing intramolecular C−H···F contacts. $N(CH_3)_2$ groups were omitted for clarity: (a) **7**; (b) **10**; (c) asymmetric unit of **12**, cation only.

suggesting that the 1,4-C_6F_4 group exerts a strong electron-withdrawing influence on *both* attached ferrocenyl groups.

This electrochemical data suggest that electronic communication between the two ferrocenyl groups through the tetrafluorophenylene spacer is weak and that complexes such as **3** and their higher oligomeric homologues do not hold promise as "molecular wires". This result was somewhat surprising, as ferrocenes linked by the corresponding unsubstituted 1,4-phenylene group, for example, (Me_5Cp)Fe(3,4-Me_2Cp)(1,4-C_6H_4)(3,4-Me_2Cp)Fe(Me_5Cp), showed significant splitting (124 mV) in the solution voltammogram.[23] This comparison suggests that either the ancillary substituents (one C_6F_5 vs seven methyl groups) or the fluorination of the phenylene spacer (C_6F_4 vs C_6H_4) weakens the electronic interaction of the two iron centers. Work is underway in our laboratories to examine each of these possibilities. Neither **7**, **8**, nor **12** showed reversible solution voltammetric behavior.

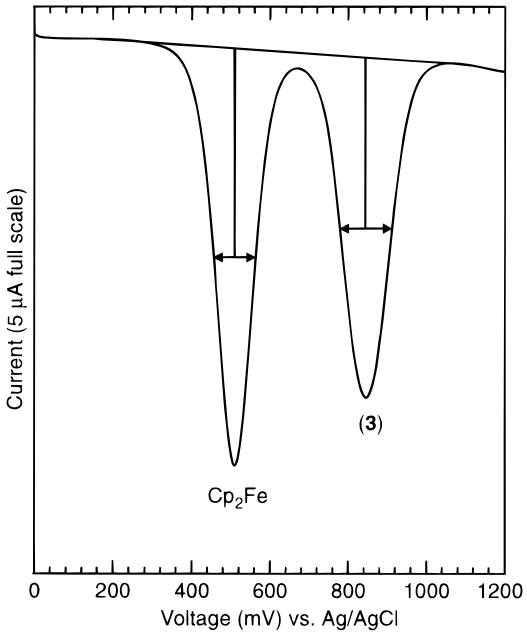

Figure 13. Square wave voltammogram of **3** showing estimation of full-width at half-maximum (fwhm) for **3** and internal ferrocene.

Conclusions. Nucleophilic aromatic substitution reactions of lithioferrocenes with hexafluorobenzene is a versatile approach to organometallic complexes in which ferrocenes are linked either to pentafluorophenyl substituents or to one another via 1,4-tetrafluorophenylene spacers. This approach enables the construction of oligomeric species via a step-growth process, although the formation of high polymers by this approach is prevented by the many side-reactions attending both the lithiation and aromatic substitution processes, as indicated by the number and quantity of byproducts observed in model reactions leading to monometallic and dimetallic species. A single dimethylaminomethyl substituent on the starting ferrocene offers improved oligomer solubility as well as planar-chirality leading to diastereomerism in 1,4-tetrafluorophenylene-linked diiron complexes. We are interested in complexes such as **8** as bidentate ligands for transition metals. Crystal structures of C_6F_5-substituted and 1,4-C_6F_4-linked ferrocenes exhibit "purposeful" arene stacking interactions as well as both "purposeful" and "diffuse" C−H···F−C interactions. We are presently examining, by experimental and computational methods, a hypothesis that the Cp−C_6F_5 interplanar torsion angles in pentafluorophenyl-substituted Cp complexes reflect electron demand by the coordinated metal fragment.

(23) (a) Bunel, E.; Campos, P.; Ruz, J.; Valle, L.; Chadwick, I.; Santa Ana, M.; Gonazlez, G.; Manriquez, J. M. *Organometallics* **1988**, *7*, 474. (b) Iyoda, M.; Kondo, T.; Okabe, T.; Matsuyama, H.; Sasaki, S.; Kuwatani, Y. *Chem. Lett.* **1997**, 35.

Experimental Section

General Considerations. All reactions were carried out using standard inert-atmosphere techniques.[24] NMR spectra were recorded on either a Varian U-400 or a Bruker AM-360 instrument. Elemental microanalysis was performed by Oneida Research Services (Whitesboro, NY) or Desert Analytics (Tucson, AZ). Melting points were obtained in open capillaries and are uncorrected. Ferrocene, (dimethylaminomethyl)ferrocene, and hexafluorobenzene were used as received from Aldrich, Strem, and PCR (now Lancaster), respectively. TMEDA was distilled from CaH_2 under nitrogen and stored over molecular sieves.

Crystallographic Studies. Crystals of **7** and of **10** were obtained by cooling concentrated hexanes solutions of the respective complexes to −5 °C. Crystals of **4** were obtained by allowing a warm, concentrated 1,2-dichloroethane solution of the complex to stand at 25 °C. Crystals of **12**·3($CHCl_3$) were obtained by dropwise addition of water to a warm, stirred suspension of **12** in methanol/chloroform until the solution became clear; subsequent filtration and cooling to −5 °C for 2 days afforded small yellow-orange prisms. Data-collection and structure-refinement information for all four complexes complexes is summarized in Table 1. Complete details of the crystallographic data collection, structure solution, and refinement are included in the Supporting Information.

Of the four complexes, the bis(methiodide) (**12**·3$CHCl_3$) warrants further discussion of crystallographic analysis. Successful refinement of this structure was plagued by residual electron density in the solvent region that could not be modeled in a satisfactory way. Attempts were made to model this disorder as both methanol and water. The residual peaks in no way resembled methanol, so this model was quickly rejected. Assignment of the residual peaks as two partially occupied oxygens of water improved the *R*-factor, but this model was deemed unreasonable, as the oxygen positions were not located within hydrogen-bonding distance of any polar residues. In the end, the three strongest Fourier peaks (3.07, 2.07, and 2.02 e^-) were not modeled in the final refinement.

Electrochemical Measurements. Single-sweep cyclic (CV) and Osteryoung square-wave (OSWV) voltammetric data were obtained for the dimeric complex **3** at a nominal concentration of 2 μM in CH_2Cl_2 using 0.10 M [*n*-Bu_4N][PF_6] as the electrolyte and activated alumina as an internal desiccant. The apparatus was a BAS 100B potentiostat with a glassy Pt working electrode, a Pt wire auxiliary electrode, and a Ag/AgCl reference electrode. The CV sweep was initialized at 0 mV, scanned to 1200 mV, and returned to 0 mV, at a scan rate of 100 mV s^{-1}. Reported $E_{1/2}$ values represent the average of two experiments. $|E_{ox} - E_{red}|$ ranged from 70 to 80 mV, and I_c/I_a was within 85% of unity, both indicators of substantially reversible oxidation. Increases in scan rate did not improve reversibility. The oxidation potential of **3** relative to internal Cp_2Fe was obtained by Osteryoung square wave voltammetry (OSWV). The cell voltage was swept from 0 mV to +1200 mV with a step resolution of 2 mV, a square wave amplitude of 25 mV, and frequency of 15 Hz. Internal resistance compensation was applied to all voltammetric experiments.

Mass Spectrometry. The direct probe EI, CI, and FAB mass spectra were obtained using a Fisons VG Quattro instrument. MALDI-TOF spectra were obtained by the Washington University Mass Spectrometry Resource.

Isolation of Dilithioferrocene (1).[12] In this context, "dilithioferrocene" (**1**) refers to the mixture of hydrocarbon-insoluble complexes obtained by treatment of ferrocene with 2.2 equiv of butyllithium and 2.2 equiv of TMEDA in hexane or pentane at 25 °C for 36 h, followed by collection of the precipitate on a filter and washing with pentane. The dilithioferrocene and TMEDA remaining in this product mixture were assayed by ^{1}H NMR in THF-d_8 solution. Triturating these mixtures with THF to remove TMEDA prior to the fluoroarylation reactions did not result in significantly different results.

Synthesis of 1,1′-Bis(pentafluorophenyl)ferrocene (2).[3] A solution of ferrocene (9.3 g, 0.050 mol), *n*-butyllithium (69 mL, 1.6 M in hexanes, 0.11 mol), and TMEDA (12 g, 0.10 mol) in hexanes (250 mL) was stirred at 25 °C for 30 h. The mixture was allowed to settle, and the supernatant was decanted with a canulla. The remaining solid was washed with an additional 100 mL of hexanes. The resulting orange solid was taken up as a slurry in 100 mL of hexanes and added, via canulla, to a stirred soltuion of hexafluorobenzene (75 g, 0.40 mol) in THF (300 mL) maintained at 0 °C using an ice bath. After the addition was complete, the reaction was stirred at 25 °C for 12 h. The volatile components were evaporated, and the resulting red residue was recrystallized from toluene/hexanes (with filtration to remove LiF and other insoluble substances). A yield of about 60% was obtained in three crops of orange-red crystals. NMR spectra were consistent with those previously published.

Synthesis of 1,4-Bis[1′-(pentafluorophenyl)ferrocen-1-yl]tetrafluorobenzene (3). C_6F_6 (0.010 mol) was added in one portion to a solution of **1** (0.010 mol) in THF (50 mL) at 25 °C. An exothermic reaction occurred with the formation of a dark precipitate. After stirring the mixture for 1 day at 25 °C, water (50 mL) was added. The precipitate was collected on a filter, washed with water, and dried under vacuum to afford 3.1 g of a red-orange solid, which was transferred to a cellulose thimble and extracted in a Soxhlet apparatus first with hexanes for 12 h. The extract was evaporated to afford 1.27 g of an orange solid. This solid was washed with hexanes (3 × 100 mL) at 25 °C to give a red residue and an orange solution. The orange solution was evaporated to afford about 20% of **2**. The red residue was recrystallized from benzene to afford about 10% of **3** as a red microcrystalline solid. An analytical sample of **3** was obtained by sublimation at 150 °C (2×10^{-5} mmHg): mp 240 °C (dec); ^{1}H NMR ($CDCl_3$) δ 4.83 (m, 4 H), 4.77 (m, 4 H), 4.56 (t, J = 2.0 Hz, 4 H), 4.43 (t, J = 2.0 Hz, 4 H); ^{19}F NMR ($CDCl_3$) δ −140.7 (d, J = 22.6 Hz, 4 F), −142.5 (s, 4 F), −159.1 (t, J = 21.4 Hz, 2 F), −164.3 (s, 4 F). Anal. Calcd for $C_{38}H_{16}F_{14}Fe_2$: C, 53.86; H, 1.90. Found: C, 53.71; H, 1.91.

Extraction of 1,1′-Ferrocenylene-1,4-tetrafluorophenylene Co-oligomers (4). The thimble residue remaining after hexanes extraction in the preparation of **3** (above) was subjected to successive 12-h extractions with other solvents. The extractor barrel was heated with an external Nichrome wire to maintain the collecting liquids near their respective boiling points. Benzene extracted 1.21 g of a red-orange solid; toluene extracted 190 mg of a red solid; chlorobenzene extracted 210 mg of a deep red solid; and 1,2-dichlorobenzene extracted 190 mg of a shiny red-brown solid. A black residue (200 mg) remained in the thimble.

Synthesis of 1-(Pentafluorophenyl)-2-(*N*,*N*-dimethylaminomethyl)ferrocene (7). A solution of *N*,*N*-(dimethylaminomethyl)ferrocene (1.22 g, 5.00 mmol), *n*-BuLi (3.5 mL of a 1.6 M solution in hexanes, 5.8 mmol), and TMEDA (580 mg, 5.00 mmol) in pentane (50 mL) was stirred for 36 h. To the resulting dark turbid mixture was added hexafluorobenzene (2.0 g, 11 mmol) in one portion, and the mixture was stirred at 25 °C for 2 h. After removal of the solvent under vacuum, the dark residue was subjected to chromatography on neutral alumina (2 × 10 cm). The first orange band was eluted with benzene and evaporated to afford 300 mg (0.733 mmol, 60%) of an orange oil, which crystallized upon standing. An analytical sample was obtained by recrystallization from hexanes at −20 °C: ^{1}H NMR ($CDCl_3$) δ 4.35 (m, 1 H), 4.28 (m, 2 H), 4.07 (s, 5 H), 3.29 (d, $^2J_{HH}$ = 13.6 Hz, 1 H), 3.09 (dt, $^2J_{HH}$ = 13.6 Hz, J_{HF} = 1.2 Hz, 1 H), 1.87 (s, 6 H); ^{19}F NMR ($CDCl_3$)

(24) Solvent purification: (a) Pangborn, A. B.; Giardello, M. A.; Grubbs, R. H.; Rosen, R. K.; Timmers, F. J. *Organometallics* **1996**, *15*, 1518. General methods: (b) Shriver, D. F.; Drezdzon, M. A. *The Manipulation of Air-Sensitive Compounds*; Wiley: New York, 1986.

δ −136.78 (d, ^3J = 21 Hz, 2 F), −157.95 (t, ^3J = 21 Hz, 1 F), −164.10 (m, 2 F); ^{13}C NMR ($CDCl_3$) δ 144.5 (d, $^1J_{CF}$ = 250 Hz, *C*F), 139.6 (d, $^1J_{CF}$ = 251 Hz, *C*F), 137.7 (d, $^1J_{CF}$ = 248 Hz, *C*F), 113.5 (td, $^2J_{CF}$ = 15 Hz, $^4J_{CF}$ = 3 Hz, C_6F_5 ipso *C*), 85.2 (*C*), 71.6 (m, *C*), 71.2 (s, *C*H), 70.1 (s, C_5H_5), 69.4 (t, J_{CF} = 4 Hz, *C*H), 68.0 (s, *C*H), 57.5 (t, J_{CF} = 3 Hz, CH_2), 44.8 (s, CH_3). Anal. Calcd for $C_{19}H_{16}F_5FeN$: C, 55.77; H, 3.94; N, 3.42. Found: C, 55.61; H, 4.02; N, 3.41.

Synthesis of 1,4-Bis[2-(dimethylaminomethyl)ferrocen-1-yl]tetrafluorobenzene (8). A solution of *N*,*N*-(dimethylaminomethyl)ferrocene (4.86 g, 20.0 mmol), *n*-BuLi (13 mL of a 1.6 M solution in hexanes, 21 mmol), and TMEDA (2.44 g, 21.0 mmol) in hexanes (100 mL) was stirred for 15 h. An orange precipitate formed. The precipiate was allowed to settle, and the orange supernatant was decanted into saturated aqueous NaCl, using an additional 50-mL portion of hexanes to wash the precipitate. The biphasic, hydrolyzed supernatant mixture was extracted with hexanes, and the organic layer was washed with brine, dried over $MgSO_4$, filtered, and evaporated to afford 1.2 g (4.9 mmol) of pure *N*,*N*-(dimethylaminomethyl)ferrocene (**5**) as determined by ^{1}H NMR analysis. This suggested that only 15.1 mmol of the desired 2-lithiated intermediate (**6**) remained in the reaction flask. To the orange solid in the reaction flask was added hexanes (100 mL) followed by hexafluorobenzene (1.4 g, 7.5 mmol) in one portion, and the mixture was heated under reflux for 2 h, cooled, and evaporated. The resulting orange residue was taken up in 100 mL of dichloromethane, filtered through Celite, and evaporated to afford 4.9 g of an orange solid. The crude product was triturated with pentane (2 × 50 mL at 0 °C) to afford 3.58 g (5.66 mol, 76%) of an orange solid, which was found by ^{1}H NMR and ^{19}F NMR analyses to comprise a 3:2 mixture of ***meso*-8** and ***dl*-8**. The combined triturant liquors were evaporated to afford 1.1 g of a waxy, orange solid, which was analyzed by ^{19}F NMR; about 45% of the integrated signal intensity corresponded to ***dl*-8** and about 40% to **7**, and the remaining signals were not assigned. The crude mixture of ***meso*-8** and ***dl*-8** was extracted with hexanes until the filtrate ran clear (10 × 50 mL with stirring). [Note: Soxhlet extraction with pentane would probably work very well for this separation.] The remaining orange filter cake was nearly pure ***meso*-8** (2.0 g, 45% yield based on C_6F_6, containing 5% of ***dl*-8** as determined by ^{1}H NMR analysis). The filtrate was evaporated to afford nearly pure ***dl*-8** (1.4 g, 30% based on C_6F_6, containing 3% of ***meso*-8** as determined by ^{1}H NMR analysis). Data for ***meso*-8**: ^{1}H NMR ($CDCl_3$) δ 4.48 (m, 1 H), 4.46 (m, 1 H), 4.40 (m, 1 H), 4.21 (s, 5 H), 3.48 (d, ^2J = 13.6 Hz, 1 H), 3.28 (d, ^2J = 13.6 Hz, 1 H), 2.01 (s, 6 H); ^{19}F NMR ($CDCl_3$) δ (referenced to internal C_6F_6 at −163.00) −138.80 (s, 4 F); {^{1}H}^{13}C NMR ($CDCl_3$) δ 85.1 (C), 72.7 (C), 71.1 (CH), 70.1 (C_5H_5) 69.4 (CH), 68.1 (CH), 57.4 (CH_2), 44.8 (NMe_2); {^{19}F}^{13}C NMR ($CDCl_3$) δ 144.5 (CF), 116.3 (C_1 and C_4 of C_6F_4), 70.1 (d, $^1J_{CH}$ = 175 Hz, C_5H_5). Anal. Calcd for $C_{32}H_{32}F_4Fe_2N_2$: C, 60.79; H, 5.10; N, 4.43. Found: C, 61.05; H, 5.05; N, 4.08. Data for ***dl*-8**: ^{1}H NMR ($CDCl_3$) δ 4.47 (m, 2 H), 4.40 (m, 1 H), 4.21 (s, 5 H), 3.46 (d, ^2J = 13.5 Hz, 1 H), 3.25 (d, ^2J = 13.5 Hz, 1 H), 1.99 (s, 6 H); ^{19}F NMR ($CDCl_3$) δ (referenced to internal C_6F_6 at −163.00) −138.65 (s, 4 F).

Isolation of 1,1′-Dilithio-2-(dimethylaminomethyl)ferrocene (9). Treatment of *N*,*N*-dimethylaminomethylferrocene with 2.2 equiv of *n*-BuLi and 1.1 equiv of TMEDA formed a dark precipitate, which was collected on a filter, washed with pentane, and dried under vacuum. The ^{1}H NMR spectrum (THF-d_8) of the resulting red solid showed several broad signals consistent with **9** containing about 1 equiv of residual TMEDA. About 20% of the integrated signal intensity was not assigned. This organolithium compound was found to be unstable over a period of a few days even when stored in our glovebox freezer (−35 °C).

Synthesis of 1,1′-Bis(pentafluorophenyl)-2-(*N*,*N*-dimethylaminomethyl)ferrocene (10). Using a canulla, a solution of freshly prepared and hexanes-washed **9** (500 mg, 1.35 mmol) in 10 mL of THF was added to a stirred solution of hexafluorobenzene (4.0 g, 21.5 mmol) in 50 mL of THF at 25 °C. The resulting red solution was stirred for 0.5 h at 25 °C, heated under reflux for 5 min, and then cooled. After removing the solvent under vacuum, the resulting dark residue was subjected to chromatography on neutral alumina (2 × 10 cm). A colorless forerun (200 mL of hexanes) was discarded. The first orange band was eluted with 1:1 CH_2Cl_2/hexanes and evaporated to afford 440 mg (57%) of an orange-red viscous oil. Crystallization from hexanes at −20 °C affored 340 mg (44%) of red crystals: ^{1}H NMR ($CDCl_3$) 4.78 (m, 1 H), 4.74 (m, 1 H), 4.44 (m, 2 H), 4.40 (m, 1 H), 4.35 (t, J = 2.0 Hz, 1 H), 3.26 (d, ^2J = 13.6 Hz, 1 H), 3.14 (dt, $^2J_{HH}$ = 13.6 Hz, J_{HF} = 1.2 Hz, 1 H), 1.83 (s, 6 H); ^{19}F NMR ($CDCl_3$) δ −136.75 (d, ^3J = 20 Hz, 2 F), −140.70 (m, 2 F), −157.27 (t, ^3J = 21 Hz, 1 F), −158.86 (t, ^3J = 21 Hz, 1 F), −163.73 (m, 2 F), −163.94 (m, 2 F); ^{13}C NMR ($CDCl_3$) δ 144.3 (d, $^1J_{CF}$ = 240 Hz, two *C*F), 139.6 (d, $^1J_{CF}$ = 250 Hz, *C*F), 138.8 (d, $^1J_{CF}$ = 245 Hz, *C*F), 137.8 (d, $^1J_{CF}$ = 250 Hz, *C*F), 137.6 (d, $^1J_{CF}$ = 240 Hz, *C*F), 113.3 (dt, $^2J_{CF}$ = 15 Hz, $^4J_{CF}$ = 4 Hz, C_6F_5 ipso *C*), 112.4 (dt, $^2J_{CF}$ = 16 Hz, $^4J_{CF}$ = 4 Hz, C_6F_5 ipso *C*), 86.2 (s, *C*H), 73.0 (s, *C*H), 72.5 (t, $^3J_{CF}$ = 2 Hz, *C*−C_6F_5), 72.4 (t, $^3J_{CF}$ = 2 Hz, *C*−C_6F_5), 72.0 (t, J_{CF} = 2 Hz, *C*H), 71.9 (t, J_{CF} = 1 Hz, *C*H), 71.5 (t, J_{CF} = 4 Hz, *C*H), 71.4 (m, *C*), 70.9 (t, J_{CF} = 5 Hz, *C*H), 57.0 (t, J_{CF} = 4 Hz, CH_2), 44.8 (s, CH_3). Anal. Calcd for $C_{25}H_{15}F_{10}FeN$: C, 52.20; H, 2.63; N, 2.43. Found: C, 52.25; H, 2.78; N, 2.43.

Isolation and Characteriation of 1,1′-(2-Dimethylaminomethyl)ferrocenylene-1,4-tetra-fluorophenylene Cooligomers (11). C_6F_6 (1.1 g, 6.0 mmol) was added to a solution of freshly prepared, hexanes-washed **7** (2.2 g, 5.9 mmol) in 40 mL of THF at 25 °C. After the initial exotherm subsided, the mixture was stirred under reflux for 2 h. After cooling the reaction and removing the solvent under vacuum, aqueous workup of the benzene-soluble red residue afforded 2.6 g of a red-orange oil, which solidified upon standing. A small portion (200 mg) was purified by column chromatography on alumina (20 mm × 10 cm). A forerun (150 mL of ether) was eluted, which was subsequently evaporated to afford about 30 mg of a red solid identified as a mixture of **7** and **10** by ^{1}H and ^{19}F NMR analysis. A dark red band was then eluted with methanol. Evaporation of the solvent afforded 0.17 g of a red solid designated as the "purified" oligomeric product **11**. A brown band remained at the top of the column. Details of the NMR spectroscopic data and end-group analysis of **11** are presented in the Supporting Information. None of the EI, CI, FAB, or MALDI spectra that we obtained for **11** showed masses higher than 2000 amu and lacked clear progressions that we could assign to the repeat unit of **11**. Evidently, the dimethylaminomethyl substituents make **11** susceptible to extensive fragmentation. Gel-permeation chromatography (GPC) experiments gave spurious results (very high elution volumes or long retention times), suggesting molecular weights of less than 500 when calibrating to polystyrene standards. In-line viscometry gave insufficient signal for an absolute molecular weight determination.

***meso*-8-Bis(methiodide) (*meso*-12).** A 20-mL test tube was charged with 101 mg (0.160 mmol) of ***meso*-8**. Methanol (5 mL) and iodomethane (2 mL) were added, and the resulting orange slurry was stirred at room temperature. No reaction was apparent. Upon boiling for 2 min, the mixture first became a clear orange solution, and then a yellow-orange precipitate separated. A second 2-mL aliquot of iodomethane was added (no visible change), and the mixture was boiled for an additional 2 min and then cooled. The yellow solid was collected on a Hirsch funnel, washed with ether, and dried in a vacuum oven at 60 °C for 4 h to obtain 132 mg (0.144 mmol, 90.2%) of a fine yellow powder: ^{1}H NMR (DMSO-d_6) δ 4.90 (m, 1 H), 4.78 (m, 1 H), 4.73 (m, 1 H), 4.67 (d, ^2J = 14 Hz, 1 H), 4.48 (s, 5 H), 4.17 (d, ^2J = 14 Hz, 1 H), 2.76 (s, 9 H); ^{19}F NMR (DMSO-d_6) −135.2 (br s). Satisfactory elemental analysis was not

obtained in two attempts. Anal. Calcd for $C_{34}H_{38}F_4Fe_2I_2N_2$: C, 44.57; H, 4.18; N, 3.06. Found: C, 43.25 and 43.26; H, 3.78 and 3.81; N, 3.15 and 2.95. The assigned structure was confirmed by single-crystal X-ray diffraction (see above).

Acknowledgment. This work was supported by the Petroleum Research Fund (30738-G1). We thank Prof. K. J. Brewer for the use of her digital potentiostat and Dr. M. R. Jordan for assistance with electrochemical experiments. We thank Prof. J. E. McGrath and Dr. Q. Ji for assistance with the GPC analyses, K. Harich for the EI, CI, and FAB mass spectra, and the Washington University Mass Spectrometry Resource for the MALDI-TOF mass spectra. We thank Prof. H. W. Gibson and Prof. M. R. Anderson for helpful discussions.

Supporting Information Available: Crystallographic data for **3**, **7**, **10**, and **12**; NMR spectral assignments and end-group analysis of **11**. This material is available free of charge via the Internet at http://pubs.acs.org.

OM990930V